

## Potential Profiles in the Central Core of the Cathode in the Star Mode Operation in an Inertial-Electrostatic Fusion Neutron Source

K. Yoshikawa 1), K. Masuda 1), H. Toku 1), A. Nagafuchi 1), T. Mizutani 1), H. Hashimoto 1), K. Nagasaki 1), Y. Yamamoto 1), K. Takiyama 2), M. Ohnishi 3), H. Matsuura 4), K. Funakoshi 4), Y. Nakao 4)

1) Inst. of Advanced Energy, Kyoto University, Uji, Kyoto 611-0011, Japan

2) Hiroshima University, Higashi Hiroshima 739-8527, Japan

3) Kansai University, Suita, Osaka 564-8680, Japan

4) Kyushu University, Hakozaki, Fukuoka 812-8581, Japan

e-mail contact of main author: kiyoshi@iae.kyoto-u.ac.jp

**Abstract.** After the successful measurements of the localized electric fields in the center-spot mode operation with relatively large space-charge effects by the laser-induced fluorescence (LIF) method, measurements of potential profiles in the star mode operation with small space-charge effects on helium gas are made in the central cathode core region of an Inertial-Electrostatic Confinement Fusion (IECF) neutron source, which is most suitable to neutron calibration in the fusion devices. Since the high-voltage is required to the star mode operation on deuterium gas, it is predicted to bring about very small beam space charge-related potential. To increase accuracy, we adopted  $n=4$  ( $2^1S$  to  $4^1D$ :HeI) transition, instead of previous  $n=3$ , which is most sensitive to the local electric fields in the Stark transition, and verified using the well-known U-shaped hollow cathode potential. The localized electric fields thus measured by LIF method using  $n=4$  transition show negligible electric fields in the star mode compared with the center-spot mode.

### 1. Introduction

As the beam-beam colliding fusion which is essential to the IECF, the most appropriate neutron calibration source for DT fusion devices, is based exclusively on the ion beam trajectories under the beam space charge-induced potential, studies of the potential profiles have been the central key issue for the past 30 years at various institutions, in particular, on the existence of the localized double well potential profiles in the central core of the cathode. In 1999, they were successfully measured directly by the laser-induced fluorescence (LIF) method [1] for the center-spot mode with a relatively large beam perveance, and potential profiles are found to be strongly dependent on the beam angular momentum in the center-spot mode (see Fig.1(lower)) running on helium gas for relatively low voltages[2]. From view point of neutron production, however, rather higher voltage is essential to increase fusion cross section, and, eventually, the star mode appears in the relatively low pressure region of glow discharge as shown in Fig.1(upper) for a hollow cathode of 50mm inner diameter, where a number of brilliant spokes due to outward electron streams are characteristic. As this mode requires higher voltages, and thus, compared with the center-spot mode, it has relatively smaller beam perveance, i.e., smaller beam-related space charge effects. This implies not distinguished potential well profiles in the central core region, and consequently, implies small optical intensity by quadrapole transition which strongly depends on the number density of  $2^1S$  HeI state (with energy level of 20.6 eV higher than the grounded state), which requires many energetic electrons to excite.

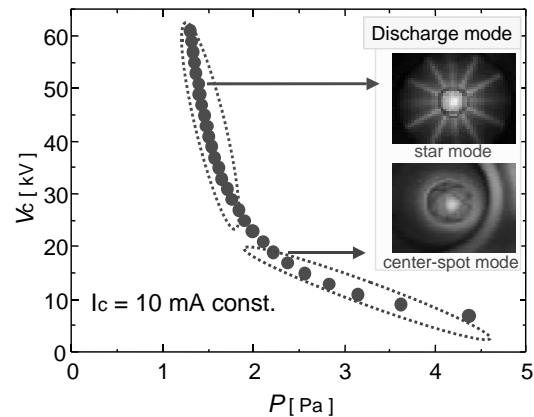


FIG. 1. Two typical IEC discharge modes (i.e., center-spot, and star) for  $I_c=10\text{mA}$ .

In order to be able to measure even relatively small electric fields as predicted in the star mode, we have applied  $n=4$  transition ( $2^1S$  to  $4^1D$ :HeI) which is more sensitive to the electric fields (about 0.1kV/cm) compared with  $n=3$  ( $2^1S$  to  $3^1D$ :HeI, about 0.5kV/cm). For verification, the well-known potential profile of the U-shaped hollow cathode is first measured.

## 2. Experimental Setup

The LIF system consists of a Nd:YAG laser (Continuum Surelite II-10-JST; 355 nm, 160 mJ) and a dye laser (Continuum ND6000; line width  $0.07 \sim 0.08 \text{ cm}^{-1}$  at 515 nm and 560 nm) with two spectrometers (Jobin Yvon TR190MS2; dispersion  $< 4 \text{ nm/mm}$ ). A polarization rotator is equipped between the dye laser and the IECF injection quartz window, and also a polarization plate between the IECF window and the spectroscop to measure the effects of polarization as is shown in Fig. 2.

In the experiments, we have chosen the IECF device with a hollow cathode, where the IECF device is spherical, made of SS304 with an inner diameter of 34 cm, and the hollow cathode of 5 cm inner diameter at the center, held by the insulator, is made of 5 mm wide curved tantalum sheets of a 0.3 mm thickness, which were precisely cut by the laser processing (Fig. 3). The laser wavelength was precisely calibrated within 1 pm through the optogalvanic effects by the galvatron (GT in Fig. 2). To measure the spatial profile, the laser injected in the  $y$ -direction was scanned horizontally in the  $z$ -direction. A He gas was chosen, and the

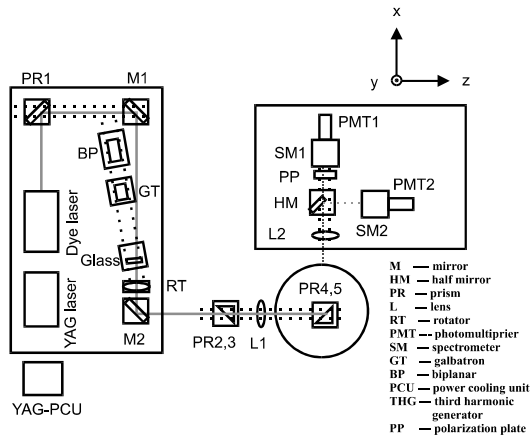


FIG. 2. Experimental setup for LIF diagnostics.



vacuum chamber : inner dia. = 340mm  
cathode grid (Ta) : inner dia. = 50mm  
outer dia. = 60mm  
thickness = 0.3mm

FIG. 3. A hollow cathode made of Ta in an IECF device.

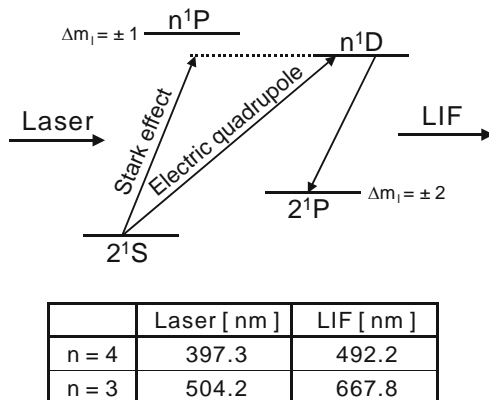


FIG. 4. Relevant energy diagram for the LIF process of HeI in electric field.

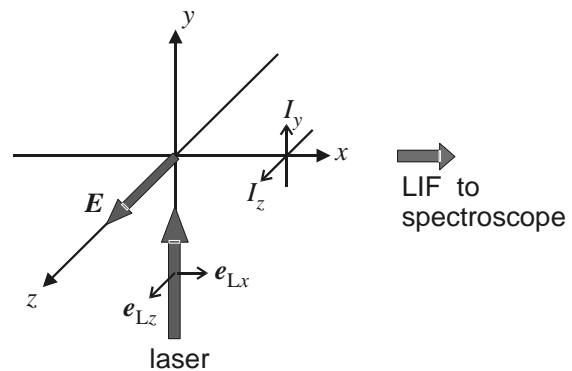


FIG. 5. Observation geometry for LIF.

metastable atoms ( $2^1S$ ) are excited to  $4^1D$  by the laser (397.3 nm) with two different polarization ( $e_{Lx}$ ,  $e_{Lz}$ ) through the forbidden transitions, i.e., the Stark-induced electric dipole moment, and electric quadrupole moment (QDP) transitions (Figs. 4 and 5) [3].

### 3. Measurement of potential profile of the U-shaped hollow cathode by Laser-Induced Fluorescence method

To verify the LIF method by  $n=4$  transition, we have chosen an U-shaped (parallel) hollow cathode as is shown in Fig.6, whose potential profile is well known. The cathode is made of two stainless steel disks of 3 cm diameter with a 1 cm gap, and applied 200V relative to the chamber with a discharge current of 5mA under the pressure of 990mTorr as is shown in Fig.6. The intensity profiles of four

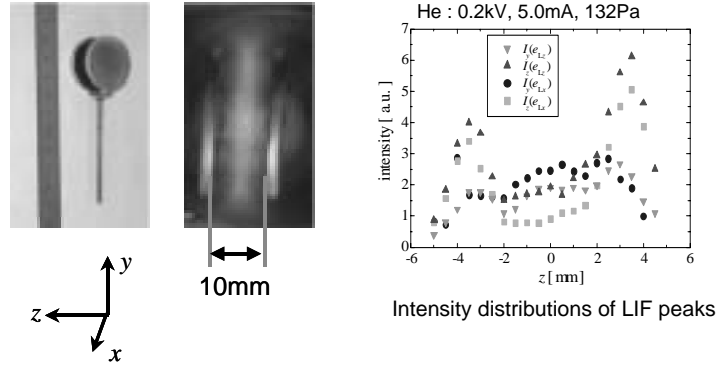


FIG. 6. A U-shaped hollow cathode with two parallel disks of 3 cm dia., and 1 cm gap, and measured LIF intensity profile.

The intensity profiles of four kinds of LIF in the z direction ( $z=0$  correspond to the center of the gap) are shown in Fig.6. It clearly indicates the strong electric fields in the vicinity of both electrode disks, whereas very small electric field near the center ( $z=0$ ) as were measured. Calculation of the electric fields from LIF profiles and their integration (potential profile) are shown in Fig.7, respectively. It is found that for  $n=4$  transition, sensitivity of electric fields less than 0.1 kV/cm is achievable. Also from derived potential profiles, the potential gap is found to be 175 V, showing good agreement with 200 V applied voltage in this experiment. It was found, consequently, excellent agreement with the experimentally obtained with high accuracy by the LIF method for  $n = 4$ .

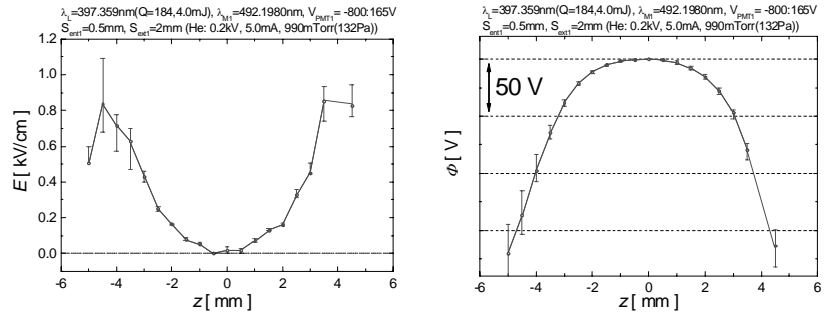


FIG. 7. Measured electric fields and potential profile of the U-shaped hollow cathode.

### 4. Electric field measurements of two discharge modes by LIF with $n=4$ transition

After verification by using the well-known potential profile of the U-shaped hollow cathode, the LIF method was adopted to measure the local electric fields in the center along the z (horizontal) axis for both the center-spot mode (5.4kV, 40mA, 5.3Pa; He), and the star mode (33.5kV, 40mA, 2.1Pa; He). Figures 8 and 9 show, respectively, a typical time evolution of LIF intensities at the core center ( $z=0$ ) of the four kinds of fluorescence, i.e.,  $I_y(e_{Lx})$  and  $I_y(e_{Lz})$  are not dependent on the electric field strength, but on the density of metastable helium atoms at the  $2^1S$  state, and among the rest of  $I_z(e_{Lx})$ , and  $I_y(e_{Lx})$ , the former depends on the Stark transition due to local electric fields, where the laser is injected with two different

polarization ( $e_{Lx}$ ,  $e_{Lz}$ ) in the y-direction, perpendicular to the z direction along which the electric fields are measured in the center (Fig. 5).

Compared with the center-spot mode in Fig.9, the electric fields for the star mode in Fig.10 have relatively large errors, and very small S/N ratio, strongly implying negligible electric fields inside the core as was predicted.

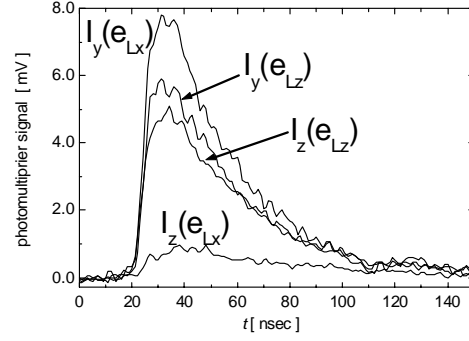


FIG. 8. Time evolutions of LIF intensities in the center ( $z=0$ ) in the center-spot mode (5.4 kV, 40 mA, and 5.3 Pa).

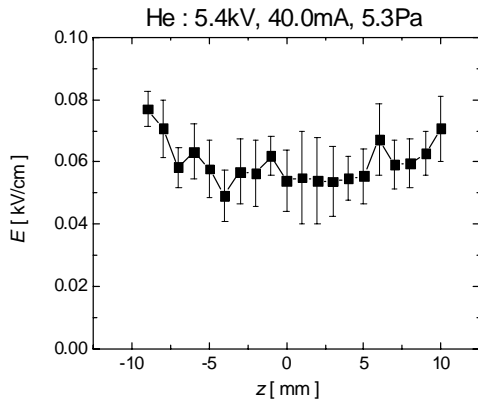


FIG. 9. Electric field profile along the z-axis in the center-spot mode (5.4 kV, 40 mA, and 5.3 Pa).

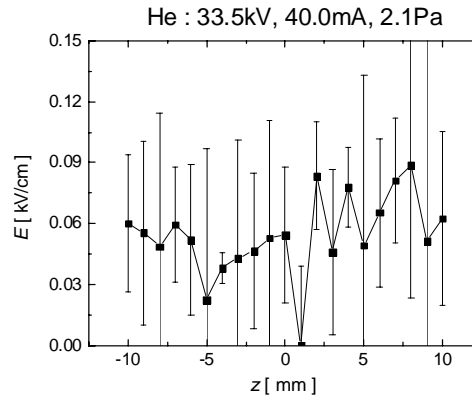


FIG. 10. Electric field profile along the z-axis in the star mode (33.5 kV, 40 mA, and 2.1 Pa).

## 5. Numerical Simulation

To analyze further, the simulation is made with assumptions that the IEC device is a weak collisional system, and the distribution functions of charged particles can be expressed by an arbitrary function of the energy  $E$  and the angular momentum  $L$  [4]. As a model equation, we introduce the following form of the ion and electron distribution functions[5];

$$f_a(E, L) = c_a \exp \left[ - \left( \frac{E - \xi_a |q\phi_0|}{\alpha\phi_0} \right)^2 - \left( \frac{L}{\beta_a L_0} \right)^2 \right], \quad (1)$$

where subscript  $a$  represents particle species, i.e. deuteron or electron, grid(cathode) voltage  $\phi_0$ ,  $L_0 = r_{cat} \sqrt{2m_a q \phi_0}$ . The cathode radius is taken as  $r_{cat} = 3\text{cm}$ . By adjusting the dimensionless parameters  $\alpha$ ,  $\beta_a$  and  $\xi_a$  values, we can simulate the broadness of the distribution functions toward energy and angular momentum directions, and slowing-down of the particles respectively. The coefficient  $c_a$  is determined by the density at the cathode, which is given by Thorson's semi-experimental expression[6]. By integrating this expression using initial value of the radial electrostatic potential profile with respect to the cathode potential, we obtain the radial profile of deuteron and electron densities, and eventually potential profiles through the Poisson equation. By using the obtained potential profile as an initial value, the process is repeated until we get a correct solution, i.e. radial profile of the potential (ion and electron density profiles). Numerical results for D: 56.6mA, 5.4kV (corresponding to the same beam

perveance of Fig. 9) and for D: 56.6mA, 33.5kV (corresponding to the same beam perveance of Fig. 10) are shown in Fig.11 for  $\alpha = 0.1$ ,  $\beta_D = 0.3$ ,  $\beta_e = 0.1$ ,  $\xi_D = 0.5$  and  $\xi_e = 1.0$ . In these parameter ranges the circulating current, i.e. deuteron density, tend to be large for small grid voltage, because of the reduced ion velocity. Thus the potential in the center core region increases for small grid voltage. It is seen that the electric fields for the center-spot mode ( $\sim 0.16$  kV/cm) is larger than the star mode ( $\sim 0.06$  kV/cm) as predicted. Although, quantitatively good agreements of experimental results with numerical results were not obtained, still the tendency of relatively smaller electric fields for the star mode compared with the center-spot mode can be seen both in the experiments and numerical results.

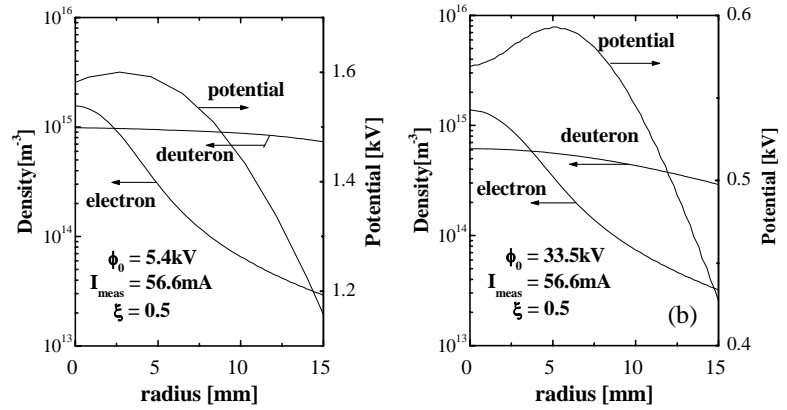


Fig. 11. Radial profiles of deuteron/electron densities and potential for (a) 5.4kV (the center-spot mode), (b) 33.5kV (the star mode) grid voltages.

## 6. Conclusions

Followed by the successful potential measurements of the center-spot mode by LIF method, potential profiles in the star mode suitable for D-D fusion are measured, and compared with the simulation results. Adoption of more electric field-sensitive  $n=4$  ( $2^1\text{S}$  to  $4^1\text{D}:\text{HeI}$ ) transition in the Stark transition shows that the localized electric fields in the star mode has small electric fields compared with the center-spot mode as was theoretically predicted.

## Acknowledgements

We would like to thank Y. Nishinosono for manufacturing various equipments, and also thank JAERI for supporting this study through Nuclear Research Promotion Program (JANP).

## References

- [1] YOSHIKAWA, K., et al., "Real time measurements of strongly localized potential profile through Stark effects in the central core region of an inertial-electrostatic fusion device", Proc. of 18<sup>th</sup> Symp. on Fusion Energy, Albuquerque, NM, Oct. 25 (2000) 27-30.
- [2] YOSHIKAWA, K., et al., "Measurements of Strongly Localized Potential Well Profiles in an Inertial-Electrostatic Fusion Neutron Source", Nuclear Fusion, **41**, (2001)717-720.
- [3] TAKIYAMA, K., et al., "Polarized forbidden-excitations by laser and electric field measurements in plasmas", Proc. of 6<sup>th</sup> Intn'l Sympo. Laser-Aided Plasma Diagnostics, Bar Harbor, Maine (1993) 43-48.
- [4] THORSON, T.A., et al., "Fusion reactivity characterization of a spherically convergent ion focus", Nuclear Fusion **38** (1998) 495-507.
- [5] NEVINS, W., "Can inertial electrostatic confinement work beyond the ion-ion collisional time scale?", Phys. Plasmas 2 (1995) 3804-3819.
- [6] MATSUURA, H., et al., "Ion distribution function and radial profile of neutron production rate in spherical inertial electrostatic confinement plasmas", Nucl. Fusion, **40** (2000) 1951-1955.